International Journal of the Physical Sciences Vol. 5(15), pp. 2278-2286, 18 November, 2010
Available online at http://www.academicjournals.org/IJPS
ISSN 1992 - 1950 ©2010 Academic Journals

Full Length Research Paper

Simulation analysis for performance of artificial water fog screening based on infrared image recognition of amphibian armored vehicles

Jun Zhi[1,2]*, Jianyong Liu[1] and Junping Shen[1]

[1]Engineering Institute of Engineering Corps, PLA University of Science and Technology, Nanjing 210007, China.
[2]Zhenjiang Watercraft College, Zhenjiang 212003, China.

Accepted 17 September, 2010

On the basis of analyzing exposed signature of amphibian armored vehicles, anti-jamming principle of dual infrared guidance and influence of water fog to infrared detection distance, the artificial water fog screening technique is put forward; and the relationship between spray quantity, water fog radius and extinction characteristics have been analyzed with Mie scattering theory which is used to choose the prime water fog radius to obtain best effect. Furthermore, a nicer performance of the water fog is proved by simulation calculation.

Key words: Amphibian armored vehicles, artificial water fog, dual infrared guidance, extinction section.

INTRODUCTION

With the rapid development of electro-optical countermeasure technology, it is difficult for guided weapons of single frequency band and mode to finish the attack mission. In order to improve the hit probability of guided weapons, developed countries have actively probed into multi-mode guided weapons. Dual infrared guided weapons (3-5, 8-14 μm wave band), with overall attack ability and stronger anti-jamming ability, are one of its developing directions.

EXPOSED SIGNATURE OF AMPHIBIAN ARMORED VEHICLES

The amphibian armored vehicles are amphibian targets of engine as the drive source. Their infrared radiation sources are mainly as follow: Top armor, air-vent shutter and spout. Take a certain type of amphibian armored vehicles as an example. Under the closest actual combat condition (atmospheric temperature is normal), the spout temperature is up to 350 to 400℃.

Suppose that the surface temperature of target is widely distributed, its average temperature is about 310K (Zhu et al., 2000). According to Wien displacement law:

$$\lambda_m T = 2898 \ \mu m.K \tag{1}$$

It can be calculated that the infrared radiation wave band of the target is fundamentally in 8 to14 μm wave band and the high-temperature part is in 3-5 μm wave band, such as the spout part, lying in the working wave band of dual infrared detectors. It forms an enormous contrast with single water background and the target's exposed signature is remarkable.

ANTI-JAMMING ANALYSIS OF DUAL INFRARED GUIDED WEAPONS

Take the typical dual infrared lead for example; it adopts the rosette scanning method to probe and recognize the targets. It not only has realized the complementation of dual wave bands in performance and function, improves anti-jamming ability, but also has the advantage of low cost, fair portability, fine trace performance etc. In addition, it has adopted the technology of dual infrared recognition, double mode tracking and computer control

*Corresponding author. E-mail: njzhijun@163.com.

and so on. Therefore, the following anti-jamming means are involved in the dual infrared lead.

Signal amplitude discrimination

Because of the existence of time variance of infrared radiation signal between interferential source and target, through different operations to the grey level array of them, the grey level variation array could be arrived and their change speed can be directly compared in time domain. In that case, the target and interferential source can be easily distinguished (Zhao et al., 2002).

Set $x_1[0,\cdots,n]$ and $x_2[0,\cdots,n]$ as two arrays, the variance array of x_1 is:

$$\hat{x}_1(i) = x_1(i) - x_1(i-1) \quad i = 1,\cdots,n \tag{2}$$

Its standard energy sum is:

$$H_1 = \sqrt{\sum_{i=1}^{n} \hat{x}_1(i)^2} \tag{3}$$

Dealt with x_2 and got H_2, H_1 and H_2 then is compared. The array with a larger fluctuation is the interferential source.

Dual infrared ratio authentication

Dual infrared ratio authentication makes use of the variance of spectral distribution between target and interferential objects to identify them.

While the instantaneous visual field of dual infrared detector sweeps double spectrum luminance on the radiation source which has the same absolute temperature, it separately produces middle and far infrared signals, and its ratio is (Liu et al., 1996):

$$k = \frac{\tau_1}{\tau_2} \frac{\int_{\lambda_1}^{\lambda_2} \frac{c_1}{\lambda^5} \frac{1}{e^{c_2/\lambda T} - 1} d\lambda}{\int_{\lambda_3}^{\lambda_4} \frac{c_1}{\lambda^5} \frac{1}{e^{c_2/\lambda T} - 1} d\lambda} \tag{4}$$

Where λ_1=3 μm; λ_2=5 μm; λ_3=8 μm; λ_4=14 μm. *S* is the object area. *T* is the object temperature. τ_1 and τ_2 are respectively atmosphere transmittance in 3-5 and 8-14 μm wave band. c_1 and c_2 are constants, $c_1 = 3.741382 \times 10^{-12} W.cm^2$

$c_2 = 1.438786 \quad W.cm^2$.

It can be found out that *k* is changed with *T*. According to interior stored dual infrared threshold, object can not only be recognized in the complicated background through dual infrared ratio, but also can prevent the interference of high temperature interferential source.

INFLUENCE OF WATER FOG TO INFRARED DETECTION DISTANCE IN EXPERIENTIAL MODEL

According to the infrared detection principle, the largest detection distance equation of infrared detector is (Hu et al., 2005):

$$R^2 = \frac{AJ\tau_A\tau_0\tau_m D^*}{(A_D\Delta f)^{1/2}K} = \left[\frac{A\tau_0\tau_m D^*}{(A_D\Delta f)^{1/2}K}\right] I\tau_A \tag{5}$$

Where *K* is SNR, D^* is the average detection ratio; *A* is the effective input aperture area of optical system; τ_0 is the transmittance of optical system; τ_m is the modulation factor; A_D is the effective area of detector; Δf is the equivalent noise bandwidth of system, above parameters are all detector parameters; τ_A is the average atmosphere transmittance; *I* is the incident radiation intensity of target into detector.

From Equation 5, it can be worked out that the largest detection distance of infrared detector principally depends on transmittance of propagating path besides the performance parameters of detector itself.

$$R = c(I\tau_A)^{1/2} \tag{6}$$

Where $c = \left[\frac{A\tau_0\tau_m D^*}{(A_D\Delta f)^{1/2}K}\right]$, is confirmed by detector system. A conclusion can be reached that it is a positive proportional relationship of the largest detection distance *R* of infrared detector to $\tau^{1/2}$.

When it passes through the water fog of which the routine length is *L*, $I' = I\tau_{fog}$ can be obtained, so the detection distance is attenuated as the following equation shows.

$$R' = R(\tau_{fog})^{1/2} = R\,\mathrm{e}^{-Gext \square L/2} \tag{7}$$

The relationship between extinction coefficient G_{ext} and water content *W* is:

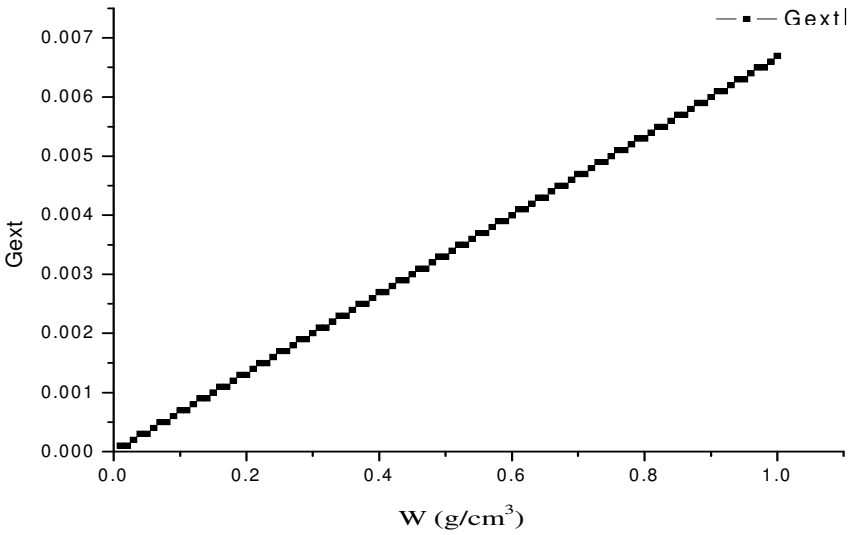

Figure 1. Extinction coefficient vs. water content (Fog with gamma distribution in thermal IR band).

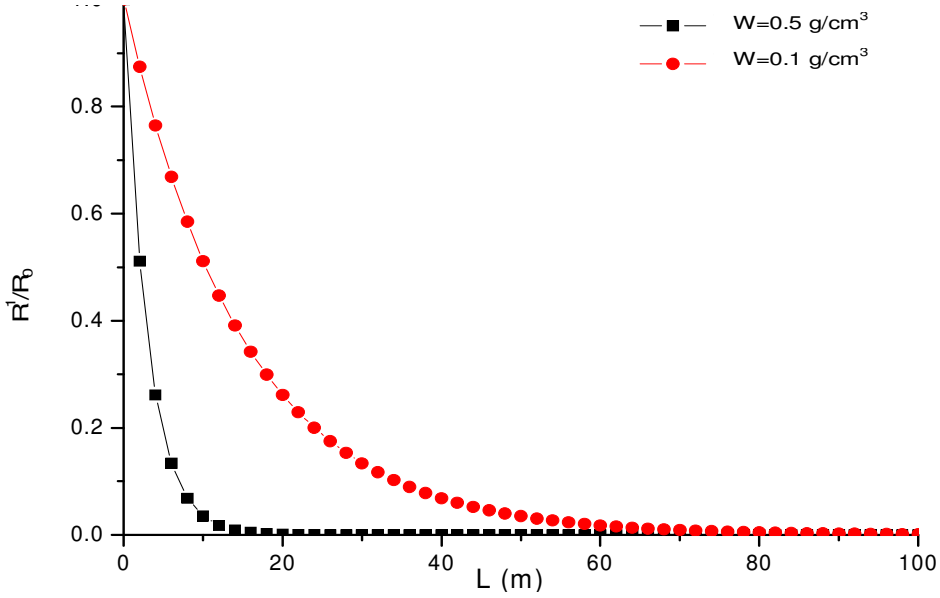

Figure 2. Sketch of detecting distance R/R0 vs. transferring distance.

$$G_{ext} = 0.0067W \quad (8)$$

Gext increase with W In Figure 1.

Taking Equation 8 into Equation 7, we can get:

$$R' = R\,\mathrm{e}^{-0.0067W \square L/2} \quad (9)$$

According to Equation 9, on the basis of the same parameters gamma distribution and 8-14 μm thermal infrared wave band range, the water content of water fog is respectively 0.5 and 0.1 g/cm^3, the propagating routine length of infrared radiation through water fog is L. The detection distance is calculated with the change of L as Figure 2 shows. In Figure 2, it can be worked out that when the water content is 0.5 g/cm^3, it decays very fast and reduces below 10% of original detection distance at the routine length of 8 m. When the water content is 0.1 g/m^3, it reduces to about 60% of original detection distance R_0 at the routine length of 8 m and about 10% of

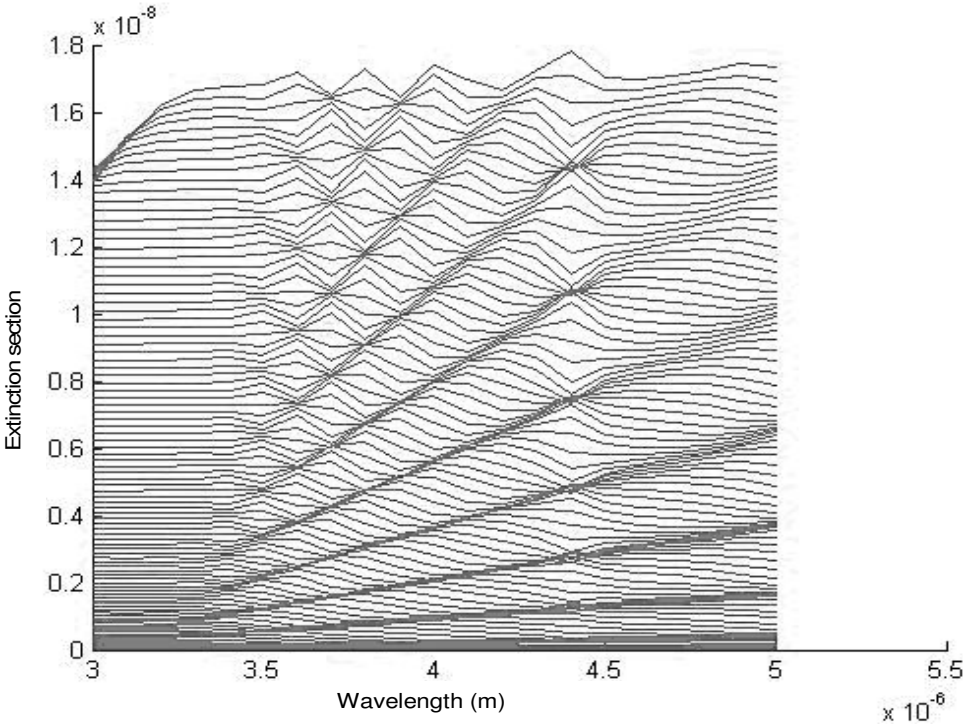

Figure 3. Extinction section of 3 to 5 μm with single water fog's radius of 0.5 to 50 μm.

original detection distance at the routine length of 34 m.

THEORY ANALYSIS OF ARTIFICIAL WATER FOG INFRARED SCREENING PERFORMANCE

Because of the surface tension effects, artificial water fog droplet is basically spherical and its droplet radius corresponds to middle and far infrared wavelength. It generates Mie scattering to middle and far infrared. The size of water fog droplet radius influences restraint effect directly. It is ascertained to design the size of water fog droplet in theory and make it reach the best screening effect under the condition of certain spraying water amount.

Provided that the refraction index of water fog droplet is $m = m_r - jm_i$, the droplet radius is *r*, incident wavelength is λ. According to Mie scattering theory, the extinction section Q_e of droplet is as Equation 10 shows (Zhao et al., 2001).

$$Q_e(m,\chi) = \frac{\lambda^2}{2\pi}\sum_{l=1}^{\infty}(2l+1)\,\mathrm{Re}(a_l + b_l) \tag{10}$$

Where a_l and b_l are Mie coefficients, they can be reached from Equation 11 and 12.

$$a_l = \frac{(\frac{A_l}{m} + \frac{l}{\chi})\,\mathrm{Re}(W_l) - \mathrm{Re}(W_{l-1})}{(\frac{A_l}{m} + \frac{l}{\chi})W_l - W_{l-1}} \tag{11}$$

$$b_l = \frac{(mA_l + \frac{l}{\chi})\,\mathrm{Re}(W_l) - \mathrm{Re}(W_{l-1})}{(mA_l + \frac{l}{\chi})W_l - W_{l-1}} \tag{12}$$

Where $\chi = \frac{2\pi r}{\lambda}$; $W_l = (\frac{2l-1}{\chi})W_{l-1} - W_{l-2}$;
$W_0 = \sin\chi - j\cos\chi$; $W_1 = \cos\chi + j\sin\chi$;
$A_l = -\frac{l}{m\chi} + [\frac{l}{m\chi} - A_{l-1}]^{-1}$; $A_0 = \cot m\chi$.

Using Matlab language to program and simulate above-mentioned equations, the extinction section of single droplet is calculated respectively whose radius is during 0.5 to 50 μm to each wavelength in 3 to 5 and 8 to14 μm wave band as Figures 3 and 4 show.From Figures 3 and 4, a conclusion can be arrived that extinction section curve is though, sometimes, partly intersects. However, on the whole when the single droplet radius is larger, the extinction curve moves upwards. Namely, in 3 to 5 and 8 to 14 μm wave band, each wavelength of extinction

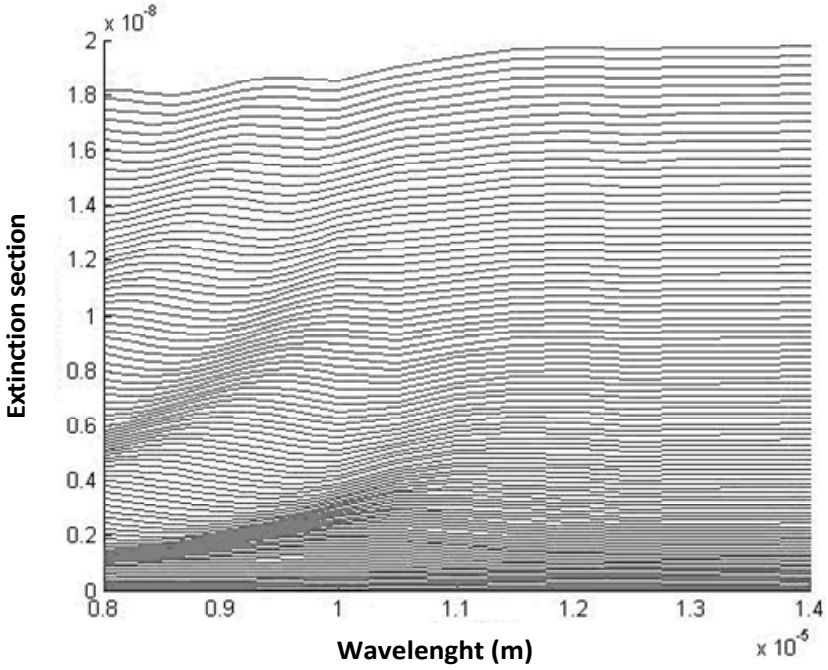

Figure 4. Extinction section of 8 ~ 14 μm with single water fog's radius of 0.5 ~ 50 μ.

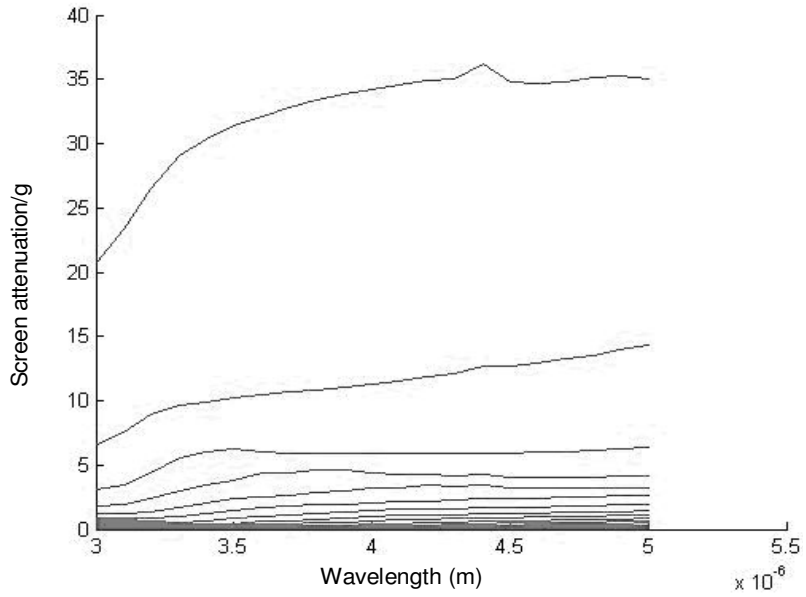

Figure 5. Screening attenuation of 3 to 5 μm with water fog's radius of 0.5 to 50 μm formed by spray quantity.

section of water fog droplet increases with the radius of water fog droplet. But to reach 3 to 5 and 8 to 14 μm for each wavelength, on the whole attenuation ability of formed water fog in unit terms of spraying water increases with water fog droplet radius decreasing. Namely, when the droplet radius is smaller, most of the screening attenuation curves move upwards (Figures 5 and 6).Through curve integral in Figures 5 and 6, the infrared screening attenuation effect of water fog can be simulated, formed by unit spray quantity and different radiuses to 3 to 5 and 8 to 14 μm wave band. Such as Figures 7 and 8 show. The smaller the water fog's droplet

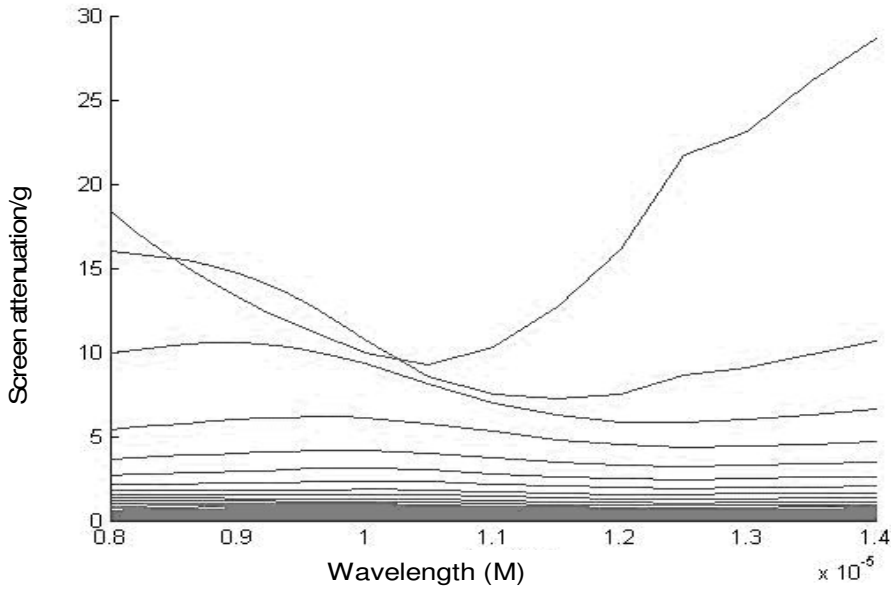

Figure 6. Screening attenuation of 8 to 14 μm with water fog's radius of 0.5 to 50 μm formed by spray quantity.

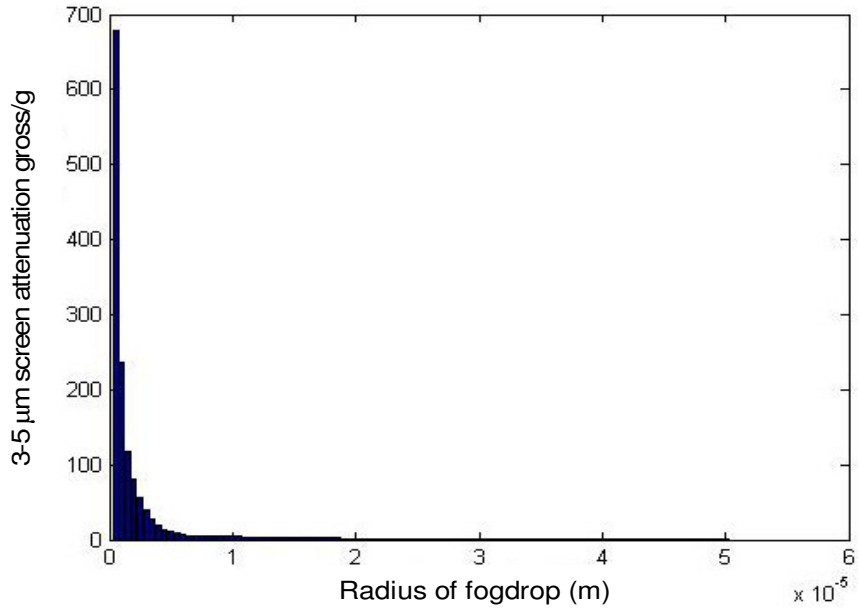

Figure 7. Screening attenuation gross of 3 to 5 μm with water fog's radius from 0.5 to 50 μm formed by spray quantity.

radius is, the stronger the infrared screening attenuation effect is; the larger the water fog's droplet radius is and the weaker the infrared screening attenuation effect is. But when the radius is much larger, to some extent, its infrared screening attenuation effect tends not to change. So, synthetically, considering actual conditions such as battlefield environment, economy and practical etc, we can control the artificial water fog droplet radius which counters 3 to 5 and 8 to 14 μm wave band in 5 to 15 μm is better.

SIMULATION TEST COMPUTATION

Suppose that artificial water fog droplet radius is 10 μm, water content is 10 g/m^3, we simulate and calculate a truss of parallel radiation penetrating into water fog screen with thickness 3 to 5 m as Figure 9 shows

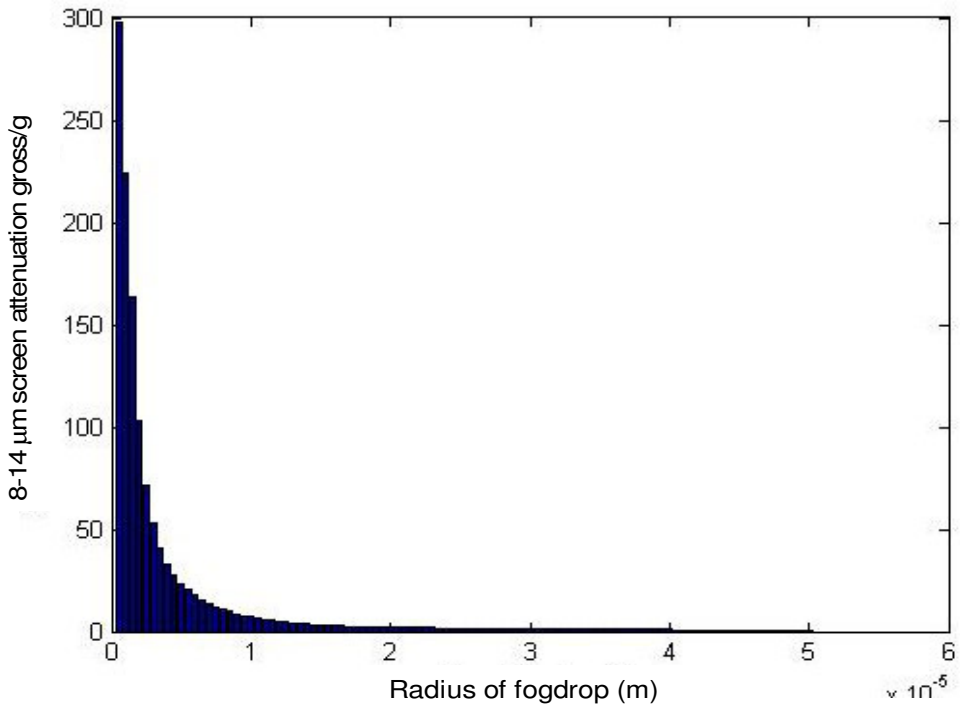

Figure 8. Screening attenuation gross of 8 to 14 μm with water fog's radius from 0.5 to 50 μm formed by spray quantity.

Figure 9. Penetration of a truss of parallel radiation into water fog screen.

(Xu et al., 2005).

$$I_t = I_0 \exp[-\int_0^L N \bullet Q_e(m,\chi)dx] \quad (13)$$

Where *N* is the density of water fog droplets: I_0 is the intensity of incident radiation: I_t is the transmission radiant intensity and *L* is the water fog thickness.

The computation result is as Figures 10 and 11 show. When water fog thickness is 3 m the screening attenuation of water fog in each wavelength of 3 to μm wave band reaches 10 dB and even 40 dB in 8 to 14 μm wave band.

Conclusions

Amphibian armored car is one of the chief weapons of landing operation. Nevertheless, dual infrared guided weapons have constituted an overwhelming threat to it. Theory analysis implies that artificial water fog can conduct the screening camouflage to the amphibian armored vehicles. On the account that early warning time

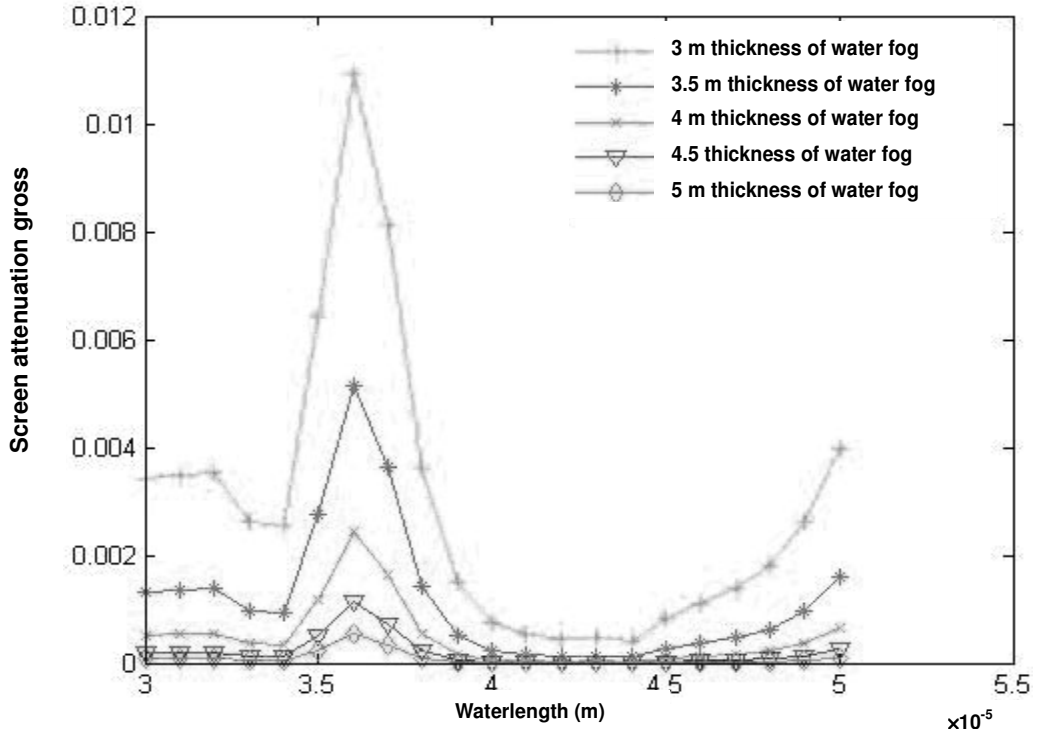

Figure 10. Attenuation of 3 to 5 μm with water fog screen's thickness from 3 to 5 m.

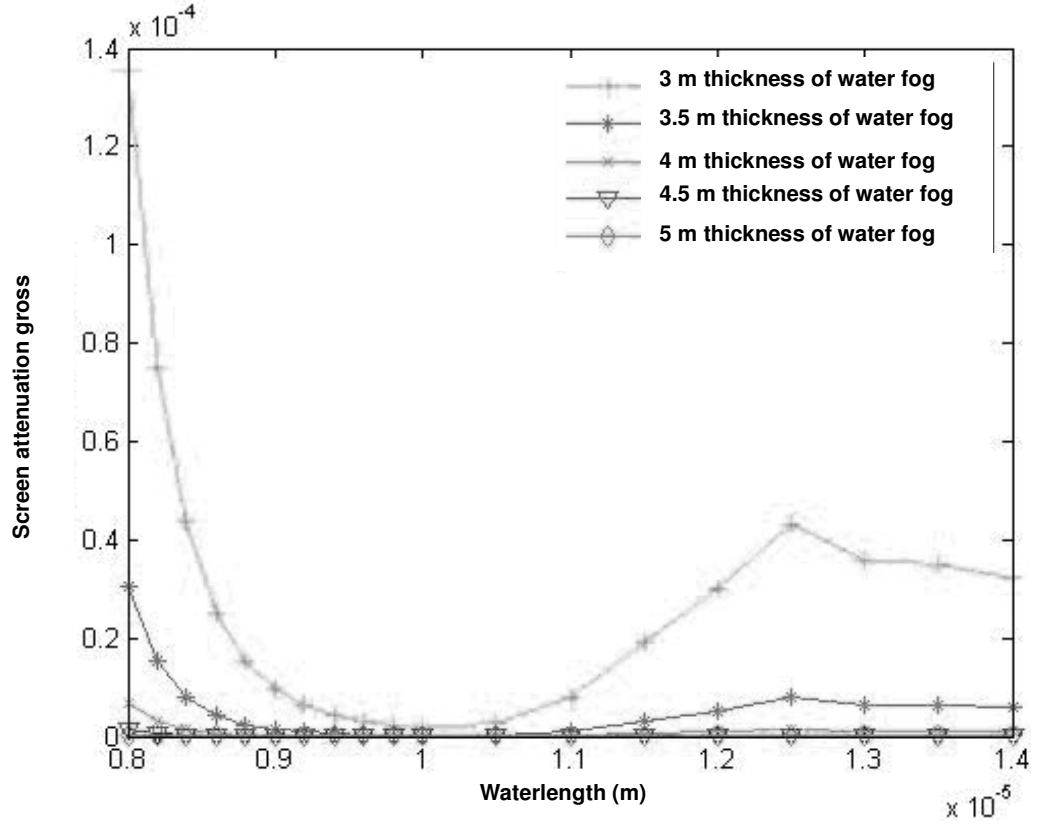

Figure 11. Attenuation of 8 to 14 μm with water fog screen's thickness from 3 to 5 m.

is longer than the time of water fog formed, water fog can counter dual infrared guided weapons effectively.

REFERENCES

Hu JH, Qin JF, Shen JP (2005). A study on camouflage approaches against infrared imaging guide. Infrared Technol., 27(2): 119-123.

Liu JH, Xu RF (1996). Study on dual spectral range IR detection. J. Beijing Institute Technol., 16(3): 292-296.

Xu B, Shi JM, Wang JC (2005). Calculation and analysis of the extinction characteristics of water fog, Infrared and Laser Eng., 34(1): 38-41.

Zhao FW, Shen ZK (2002). Study on simulation of infrared decoy recognition: gray-scale time sequence analysis. Infrared Laser Eng., 31(4): 286-288.

Zhao ZW (2001). Study on radio wave propagation characteristics and remote sensing of hydrometeors, 5(1): 29-31.

Zhu SY, Wei DM, Yao JT (2000). Research on MBT and infrared irradiation characteristics with ground-object background. Infrared Technol., 22(5): 45-50.